Jan. 2014, Volume 8, No. 1 (Serial No. 74), pp. 73-88
Journal of Civil Engineering and Architecture, ISSN 1934-7359, USA

Pseudo-Dynamic Testing for Seismic Performance Assessment of Buildings with Seismic Isolation System Using Scrap Tire Rubber Pad Isolators

Huma Kanta Mishra[1], Akira Igarashi[2], Dang Ji[2] and Hiroshi Matsushima[2]

1. Department of Urban Management, Kyoto University, Kyoto 615-8540, Japan

2. Department of Civil and Earth Resource Engineering, Kyoto University, Kyoto 615-8540, Japan

Abstract: Investigation of seismic performance of buildings with STRP (scrap tire rubber pad) seismic isolators by means of pseudo-dynamic tests and numerical simulation is presented. The isolated building is numerically modeled, while the base isolation layer is considered as the experimental substructure in the pseudo-dynamic tests. The test result verifies that the STRP isolator shows acceptable shear deformation performance predicted by the design methods, and demonstrated that seismic isolation using STRP works as a protective measure to provide enhanced seismic performance of the building indicated by the reduction of top floor absolute acceleration, drift and base shear as designated.

Key words: Pseudodynamic test, STRP isolator, numerical simulation, base isolation, seismic performance.

1. Introduction

Base isolation systems are being employed in several earthquake-prone areas in the world to design new buildings and to retrofit existing building structures [1]. Application of this attractive technology is limited to important and valuable structures. One of the reasons for this situation is the size, weight and incurred cost of the base isolation devices [2]. It should be noted that commercially available base isolation devices are far from the reach of a poor family in developing countries. A reduction in the weight and cost of seismic isolators would permit a significant increase in their application to many ordinary residential and commercial buildings [3].

Several studies have been conducted using either steel laminated rubber bearing [4] or fiber-reinforced elastomeric isolators [2, 3, 5] as low cost base isolation systems for structures in highly seismic regions in the world. These types of seismic isolators are still economically unacceptable considering the purchasing capacity of poor families in, for example, the South Asian region. The solution of the above issues shall be the development of base isolation systems which can be effective in reducing the seismic demand of the structures and are made of easily available materials at an affordable cost.

As an economical and easily available option for the base isolation system, the use of STRP (scrap tire rubber pad) as seismic isolators has been proposed [6]. The STRP layers are fabricated by cutting out rectangular-shaped rubber pads from the tread part of scrap tires. Due to the strain constraining effect of steel reinforcing cord layers embedded in the rubber pad, STRP is expected to show high stiffness in axial compression and supporting load capacity along with a high level of flexibility and deformability in lateral shear, which are suitable to the requirement for the character of seismic isolators. The authors conducted analytical and experimental study by means of loading tests in static compression and shear in order to evaluate the mechanical properties of layer-unbonded

Corresponding author: Huma Kanta Mishra, Ph.D., research field: structural dynamics lab. E-mail: Mishra.kanta.34a@st.kyoto-u.ac.jp.

and layer-bonded STRP samples for the purpose of isolation device [7, 8].

Prior to their application in real building structures, it is essential to assess how the base isolated building with STRP isolators responds to dynamic loading. When the response characteristics of a structural system are not well understood or do not permit numerical modeling, physical testing provides the only accurate method to analyze the dynamic response of the structure [9]. The two main methods currently used to test the structures under the influence of dynamic loading are the shake table test and the pseudo-dynamic testing method [10]. Small-scale models of structures have to be used in shake table tests because of the limited size and capacity of the available shake tables and therefore it is often difficult to investigate the behavior of full scale structures. The other problem associated with testing of the reduced scale model is that the scale effect which may cause misleading of the test results [11]. The pseudo-dynamic testing approach can be used to avoid the limitations of the shake table test along with the scale effects for evaluating the performance of large scale structures under earthquake loads. In addition, it is not necessarily required to test the complete structure: An experimental test on a key part of the structure can provide a better understanding of the whole structural response [12]. In pseudo-dynamic testing, a critical nonlinear structural element that cannot be modeled satisfactorily is tested physically while the remaining part of the structure that can be modeled with confidence is modeled with a numerical formulation. The former and the latter are referred to as the experimental substructure and the numerical substructure, respectively, in the substructuring technique, which is a combination of numerical simulation and experimental test on a subpart of the structure which can be regarded as the better understanding of the entire structural response [12]. The loading of the experimental substructure is conducted by using hydraulic actuators to apply the target displacements to the experimental specimen. The restoring force of the experimental substructure recorded from the load cell of the actuators and that of the numerical parts are integrated in parallel into dynamic equation of equilibrium of the entire structure [13].

In this work, seismic performance of STRP seismic isolators is investigated by means of pseudo-dynamic testing using a hypothetical three-story concrete frame building model. The three-story building is represented by a 3-DOF model with lumped mass at each floor level and the lateral stiffness of each story represented by an elastic shear spring. With an additional DOF (degrees of freedom) assigned for the base isolation floor, the structure is modeled as a 4-DOF system. The base isolation system is considered as the experimental part while the superstructure is considered to be the numerical part. The STRP isolators were fabricated as scale models of a hypothetical prototype isolator with a scale factor of 1/3 due to the capacity of the testing equipment available. In order to evaluate the seismic performance of a building with STRP isolator application, two levels of external seismic excitations were used to evaluate the seismic performance of the building. For this purpose, input accelerograms with the amplitude of 1940 Imperial Valley Earthquake El Centro record multiplied by 1.0 and 1.5 were used as the input. The pseudo-dynamic test results were compared with numerical simulation results to validate the simulation results. These test results were further compared with the numerical simulation results for the fixed base building to evaluate the seismic response performance of the purposed base isolation system.

2. STRP Isolator

The STRP specimens were prepared according to the steps as outlined in Refs. [14-16]. As illustrated by Fig. 1, STRP samples were fabricated by cutting out square shape pads of dimensions 100 mm × 100 mm × 12 mm from the tread part of the tires. The tire product used for the preparation of STRP specimen samples in this study is Bridgestone Tire, 385/65R22, 5. Each layer of

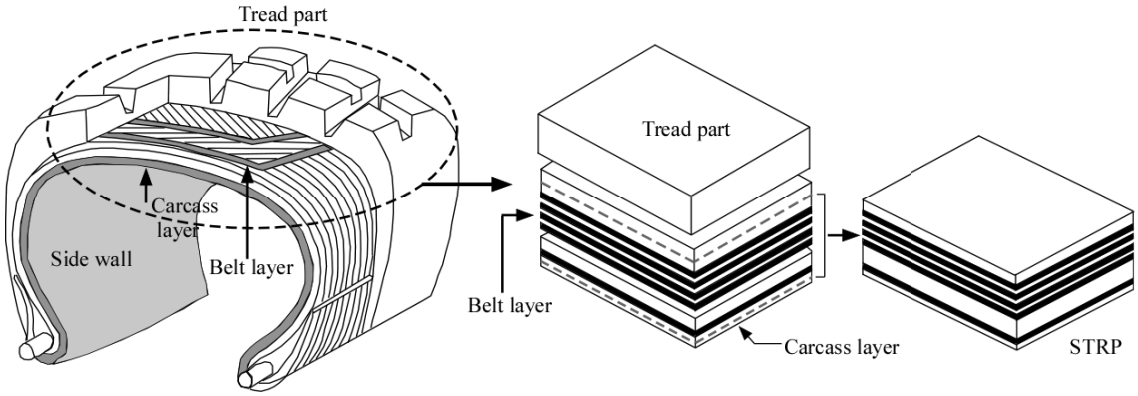

Fig. 1 STRP preparations using the tread part of the tire.

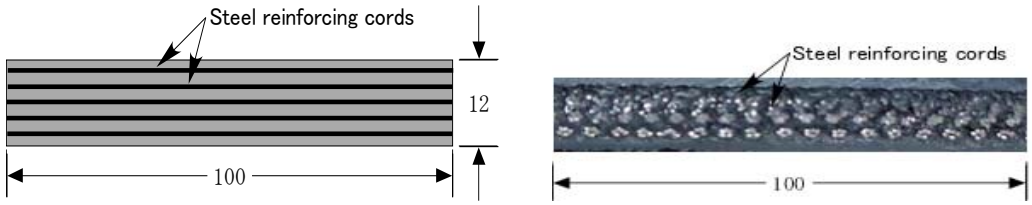

Fig. 2 Cross section of a single layer STRP: sketch and photograph.

STRP isolator shown in Fig. 2 includes five layers of steel reinforcing cords, comprising a number of strands in twisted form and embedded in the rubber material in interleaved orientations.

The raw STRP samples taken from a tire are sanded using a belt sanding machine, so that smooth plain surfaces are obtained on the STRP samples, and the surfaces are cleaned to achieve proper good quality adhesion between the surfaces. The chemical treatment of the surfaces by applying the Chemlok 7701 primer (Lord Corp.) with a brush improves compatibility with adhesive and environmental resistance, thus making the rubber surfaces more receptive to bonding. The bonding between STRP samples is conducted immediately after the solvent has flashed off to achieve the best adhesion quality in creating layer-bonded STRP samples.

The Fusor 320/322 (Lord Corp.) is used as the epoxy adhesive containing resin and hardener compounds. The adhesive is prepared as recommended by the manufacturer for general purpose (temperature range between -40 ^{o}C to 204 ^{o}C) application, and is applied on both sides of STRP surfaces using a spatula with a target thickness of 0.5 mm. Four STRP samples are assembled into a layer-bonded STRP and pressure (about 0.2 MPa) is applied. The layer-bonded STRP samples are placed undisturbed for 24 h to achieve fully cured. The isolator specimen prepared in this manner is referred to as STRP-4 in this study. Fig. 3 shows the process of surface preparation, adhesive application and cured samples. The dimensions of the STRP-4 are shown in Table 1, and the material properties of the STRP sample are presented in Table 2. The rubber has shear modulus of 0.89 MPa and hardness of 60 Durometer [17, 18].

The prototype isolator is assumed to be designed with plan dimensions of 300 mm × 300 mm and overall thickness of 150 mm. The thickness of the isolators, corresponding to twelve layers of STRP, is specified considering to achieve the target displacement capacity at shear strain of 1.55 (based on the thickness of rubber). The STRP-4 isolator specimens with plan dimensions of 100 mm × 100 mm can be interpreted as 1/3 scale models of the prototype STRP isolators.

The type of similitude law to be applied to the small-scale models depends on the aim and methodology of the test. For a dynamic problem, if

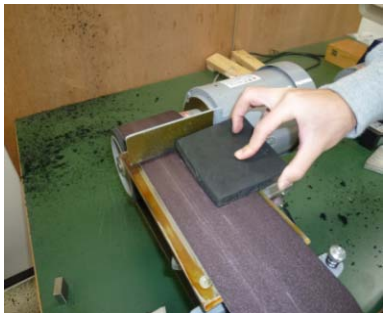
(a) Sanding of a STRP layer


(b) Single layer with adhesive on surface


(c) Fully cured STRP-4 samples

Fig. 3 Preparation of STRP-4 specimen.

Table 1 Geometrical properties of STRP-4.

Dimensions of a single layer	100 mm × 100 mm × 12 mm
Thickness of steel reinforcing cords	0.4 mm
Adhesive	2 mm
Total thickness	50 mm
Nominal rubber thickness t_r	40 mm

mass (M), length (L) and time (T) are selected as the three basic dimensions, then all the variables involved in the dynamics can be derived from them [19]. The similitude law used for the pseudodynamic test in this study is shown in Table 3.

3. Quasi-Static Tests

3.1 Loading System

The schematic view of the loading system used to carry out the quasi-static loading tests, as well as the substructure pseudo-dynamic test, is shown in Fig. 4. This loading system consists of one, three and five actuators in the x, y and z directions, respectively. In all the directions, each actuator is pin-connected to the reaction frame and to the rigid loading block. These three actuators, namely, FX, FY and FZ actuators are used to apply displacement and force in the respective directions. In addition to these actuators, four actuators are used to control the rotation with respect to x and y axes and the remaining two actuators are used to control the rotation with respect to z axis. The specimen isolator is placed between the two steel plates attached to the reaction frame and the loading block to represent the superstructure and substructure, respectively. No fastening system was used to connect the specimen with the support surfaces. The capacity of the loading system is shown in Table 4.

3.2 Test Procedure

Prior to the pseudodynamic tests, two quasi-static cyclic loading tests were performed to investigate the fundamental properties of the STRP isolator. The constant vertical axial pressure of 10 MPa and 5 MPa was applied for the two tests, which are referred to QS10 and QS5 hereafter, respectively. The specimens were loaded vertically with a constant load by the load-controlled vertical actuator FZ, and a series of

Table 2 Material properties.

Parameters	Values
Shear modulus G (tire rubber)	0.89 MPa
Young's modulus E (steel cords)	200 GPa
Poisson's ratio υ (steel cords)	0.3

Table 3 Similitude law for dynamic problem.

Physical quantity	Dimension	Scale factor
Length	L	S
Time	T	S
Mass	M	s^3
Velocity	LT^{-1}	1
Acceleration	LT^{-2}	s^{-1}
Displacement	L	S
Force	MLT^{-2}	s^2
Stiffness	MT^{-2}	S

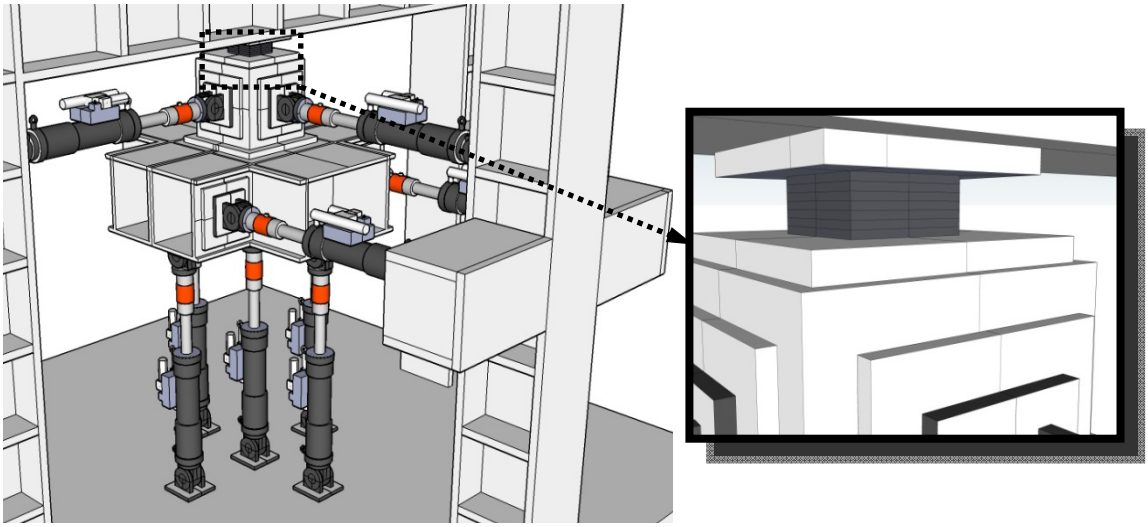

Fig. 4 Schematic view of loading system.

Table 4 Capacity of testing facility.

Actuator	Max. displacement (mm)	Max. load (kN)	Direction	Notation
No. 1	±100	±500	Vertical	*FZ*
No. 2	±100	±100	Horizontal	*FX*
No. 3	±100	±100	Horizontal	*FY*

horizontal cyclic displacements were applied with the horizontal actuator FX. The horizontal actuator FY was utilized to constrain the out-of-plane movement of the loading block.

For the QS10, the 1/3 scale model isolator was tested in cyclic shear with three fully reversed cycles at three maximum shear displacement amplitudes of 20, 40 and 60 mm, corresponding to shear strain of 50%, 100% and 150%, respectively. Similar procedure was followed for the QS5, except that the test was conducted with reduced displacement amplitudes of 15, 30, 45 and 60 mm which correspond to shear strain of 37.5%, 75%, 112.5% and 150%, respectively. The test results of QS10 and QS5 were used to determine the mechanical properties of the specimen including stiffness and equivalent damping ratio. As a representative test result, lateral load-displacement obtained by test QS5 is shown in Fig. 5. Detailed result of quasi-static loading test of STRP-4 specimen is described in Ref. [8].

3.3 Parameter Identification

The effective stiffness and equivalent damping ratio of the tested STRP isolators were determined by the quasi-static loading test results. The target fundamental period of the isolation system was determined considering the stability and acceptable displacement capacity. The required parameters were determined to achieve the target period of 1.8 s. First of all, the test results of QS5 and QS10 were plotted, and then the relationship between effective damping and shear strain for 3.3 MPa axial pressure was predicted. The relationship between the equivalent damping ratio and shear strain for different levels of axial pressures is shown in Fig. 6. The predicted equivalent damping ratio under the 3.3 MPa axial pressure at 120% shear strain is approximately 0.11. A similar technique was adopted to predict the effective stiffness of the tested isolators. The relationship between effective stiffness and shear strain for different level of axial pressures is shown in Fig. 7. This figure shows that the variation of effective stiffness is not significant. The predicted

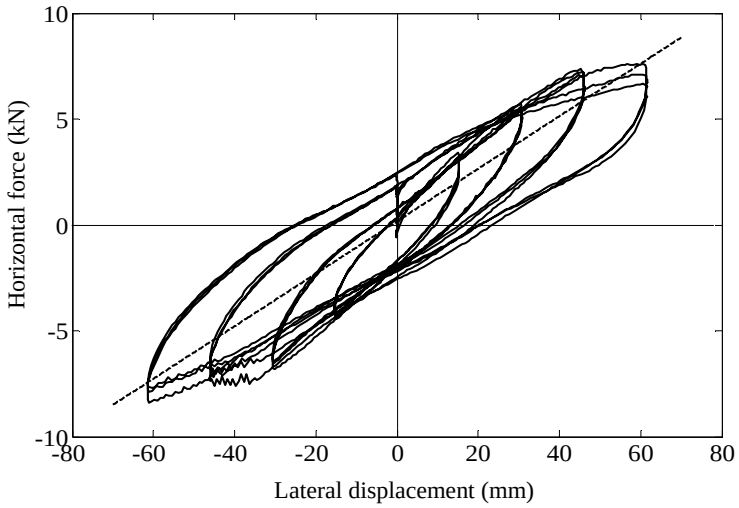

Fig. 5 Load-displacement plot for quasi-static loading of STRP-4 with axial pressure of 5MPa (QS5).

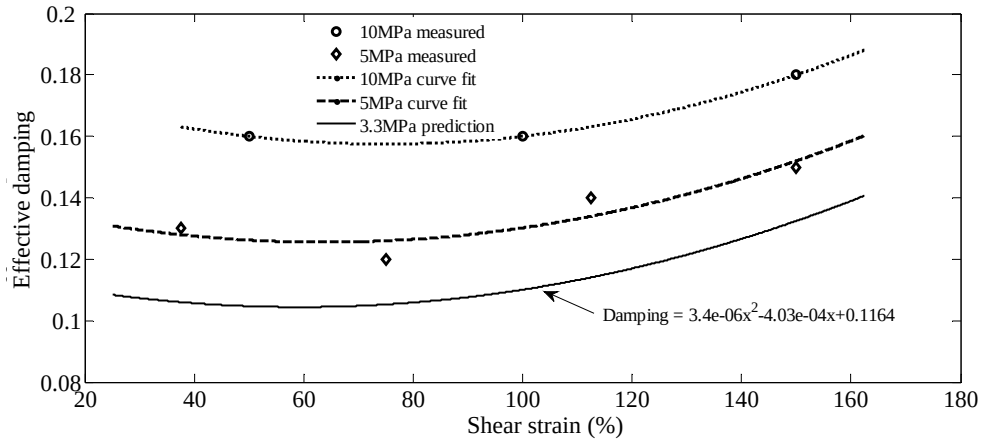

Fig. 6 Relationship between equivalent damping ratio and shear strain amplitude for different levels of axial pressure.

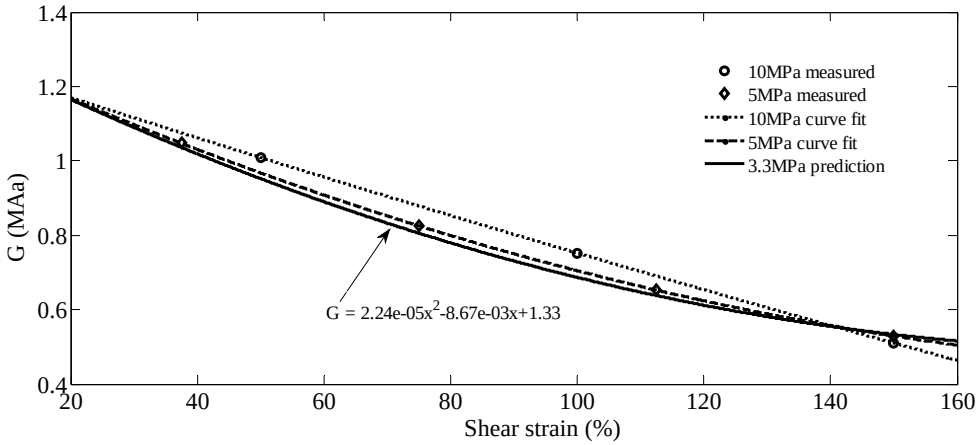

Fig. 7 Relationship between equivalent stiffness and shear strain amplitude for different levels of axial pressures.

effective stiffness for 3.3 MPa axial pressure at 120% shear strain is approximately 122.4 kN/m. The equivalent damping ratio and effective stiffness are used in numerical dynamic response analysis of the

structural model as described later.

4. Pseudo-Dynamic Tests

4.1 Building Model

A series of pseudo-dynamic tests were conducted on the hypothetical numerical model of a three-story reinforced concrete moment-resisting frame structure building with brick masonry infill walls isolated by STRP isolators to simulate the structural seismic response involving STRP isolators and to verify the efficiency. The building with dimensions of 7.85 m by 11.25 m in plan and 9.0 m in height, shown in Fig. 8a, was designed in based on the provisions of NBC (Nepal Building Code) [20] and UBC 1997 (Uniform Building Code 1997) [15]. All the columns are of a square cross section of 300 mm by 300 mm and all the beams are of 230 mm in width and 350 mm in depth. A floor slab is added at the ground level to provide physical separation between the substructure and superstructure. The building was designed on a stiff soil site with the seismic zoning factor of 1.0 as per NBC. For the analysis of the fixed-base building, the infill walls were not included in the lateral force resisting system. The weight of the structure including 25% for seismic design is approximately 4,396 kN. The fundamental period T_t of the fixed-base structure was calculated to be equal to 0.31 s by using the Eq. (1) given in NBC. The fixed-base period of the building is approximately 0.51 s.

$$T_t = 0.06\,H^{3/4} \tag{1}$$

where, H is the height of the building in meter.

There are a total of 15 STRP isolators that are installed under each of the columns. The STRP isolators were assumed as designed to be applied to the building in accordance with the building column loads with the loading combination 1.2 DL + 1.0 LL + |E| as in UBC, 1997 [15]. The average axial compressive pressure on an isolator is approximately 3.3 MPa, although the axial compressive pressure varies depending on the location of the isolator. The size and thickness of the isolators were computed so that 1.8 s base isolation period is achieved. The equations of motion were formulated for the entire structure with base isolation, represented as a 4-DOF system, as shown in Fig. 8b. The mass and stiffness properties of the building are shown Table 5. The stiffness properties were computed excluding the brick masonry infill walls.

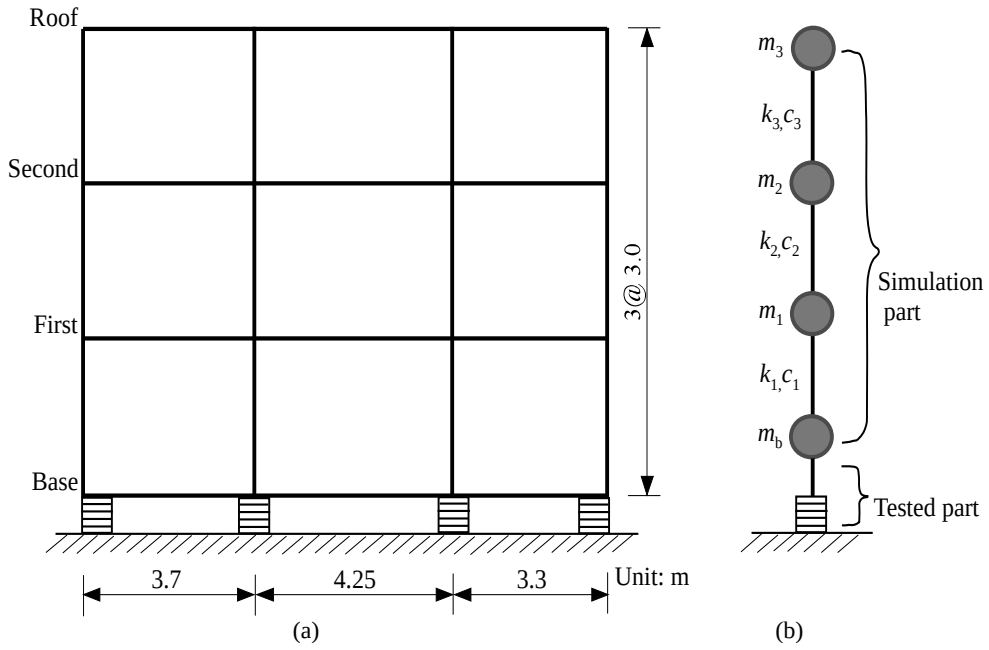

Fig. 8 Model of building with base isolation: (a) basic dimensions; (b) division into simulation and experimental parts.

Table 5 Mass and stiffness properties of building model.

Level	Mass (t)	Horizontal stiffness (kN/mm)
Base	85.0	5.5
First	127.6	87.1
Second	127.6	87.1
Roof	108.2	87.1

4.2 Control System

The control system shown in Fig. 9 was used to conduct the substructure pseudo-dynamic tests in this study. This control system consists of: (a) test control PC equipped with AD/DA interfaces; (b) loading system control PC; (c) digital servo controllers with instrumentation panel; (d) hydraulic loading system. The test control PC conducts numerical time integration of the equations of motion and is connected with the servo controller.

4.3 Algorithm of Substructure Pseudodynamic Test

A numerical time integration scheme using the prediction-correction procedure was implemented to the test control PC.

In this study, the structural system is considered as a MDOF (multi-degree-freedom) system. The isolation floor displacement is designed as the first DOF as

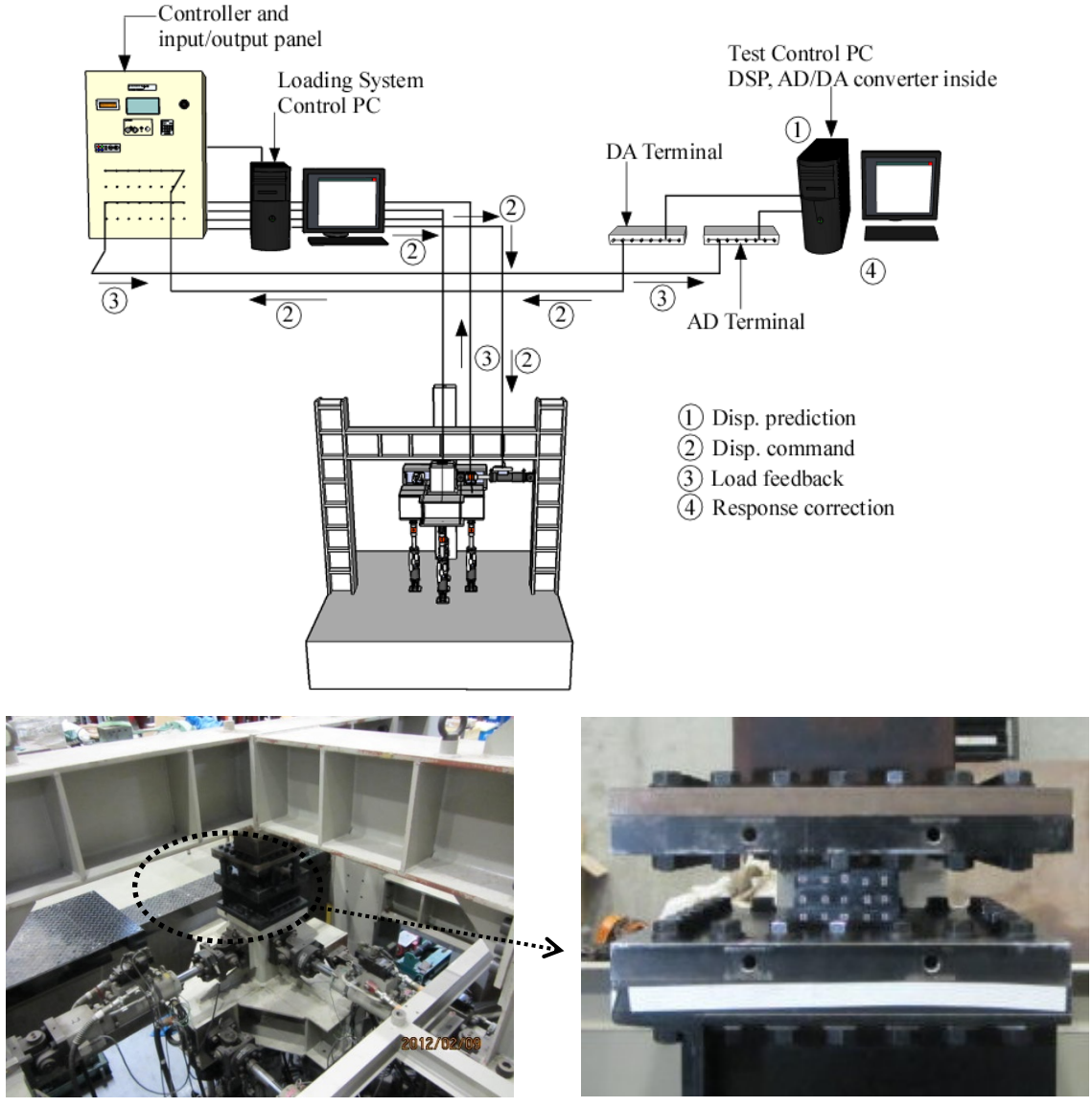

Fig. 9 Test system and specimen for substructure pseudo-dynamic tests.

represented by the first component of the displacement vector $\{x\}_1$. After imposing the displacement in the next step $\{\tilde{x}_{n+1}\}_1$ to the STRP isolator specimen, the measured restoring force f_{n+1} is used to evaluate the correction force increment vector $\{\Delta f_c\}$, which is the difference between the restoring force based on the initial elastic stiffness and the actual load. The correction force increment vector for the isolation floor can be expressed by Eq. (2).

$$\{\Delta f_c\}_1 = f_{n+1} - f_n - k_1(\{\tilde{x}_{n+1}\}_1 - \{x_n\}_1) \quad (2)$$

where, f_n is the restoring force of the experimental substructure in the previous step, k_1 is the elastic stiffness of the shear spring 1 in the MDOF system.

Accordingly, the procedure used to calculate the response at time $(n+1)\Delta t$ can be outlined as below:

Step 1: Calculate the response displacement vector at the next step $\{\tilde{x}_{n+1}\}$ for the entire structural model using Eq. (3):

$$\{\tilde{x}_{n+1}\} = \{x_n\} + \Delta t\{\dot{x}_n\} + 0.5\Delta t^2\{\ddot{x}_n\} + \beta[\hat{M}]^{-1}\{\hat{f}\}\Delta t^2 \quad (3)$$

where,

$$[\hat{M}] = [M] + 0.5\Delta t[C] + \beta\Delta t^2[K] \quad (4)$$

$$\{\hat{f}\} = [M]\{1\}\ddot{z}(t) - \Delta t([C] + 0.5\Delta t[K])\{\dot{x}_n\} - \Delta t[K]\{\dot{x}_n\} \quad (5)$$

Step 2: Apply the predicted displacement of the experimental substructure $\{\tilde{x}_{n+1}\}$ as the target displacement command to the loading system.

Step 3: Measure the feedback restoring force f_{n+1} from the experimental substructure.

Step 4: Calculate the corrected displacement using Eq. (6):

$$\{x_{n+1}\} = \{\tilde{x}_{n+1}\} - \beta[\hat{M}]^{-1}\{\Delta f_c\}\Delta t^2 \quad (6)$$

If the correction part $\beta[\hat{M}]^{-1}\{\Delta f_c\}^{-1}\Delta t^2$ is sufficiently small, then compute the velocity and acceleration by Eqs. (7) and (8), respectively, and proceed to the next step, otherwise, substitute $\{x_{n+1}\}$ as predicted displacement $\{\tilde{x}_{n+1}\}_1$ and go back to Step 2.

$$\{\dot{x}_{n+1}\} = \{\dot{x}_n\} + 0.5(\{\ddot{x}_n\}) + \{\ddot{x}_{n+1}\}\Delta t \quad (7)$$

$$\{\ddot{x}_{n+1}\} = \{\ddot{x}_n\} + [\hat{M}]^{-1}(\{\hat{f}\} - \{\Delta f_c\}) \quad (8)$$

The convergence tolerance is selected depending on the finite resolution of the loading control system and measuring devices. There are merits and demerits of using a small convergence tolerance limit, and of using a large one. In this test, the displacement tolerances were set as 0.1 mm.

4.4 Test Program and Result

For the purpose of the pseudo-dynamic test, NS component of the El Centro record of 1940 Imperial Valley Earthquake (Fig. 10) and the accelerogram scaled with the factor 1.5 were used as the seismic input to the building model shown in Fig. 8.

In this study, the pseudodynamic tests of the specimen isolator were conducted under a constant vertical axial pressure of 3.3 MPa. The seismic responses of the prototype model obtained by the pseudodynamic tests were compared with the simulation results with respect to the top floor absolute acceleration, top floor drift, isolator's displacement and base shear transmitted to the superstructure. Fig. 11 shows the force-displacement relationship of the isolator obtained from the pseudo-dynamic tests using 100% and 150% El Centro records for shear strain levels of 70% and 100%. The corresponding deformed state of the STRP isolator is shown in Fig. 12. These shear strains are well within the deformation capacity of the STRP-4 specimen of approximately 150% obtained by the quasi-static loading test.

5. Numerical Dynamic Analysis

The numerical dynamic analysis of the building isolated with the STRP isolators was carried out using the MDOF model shown in Fig. 8b, in which the hysteretic behavior of the STRP seismic isolator is modeled as a combination of a linear spring and viscous damping determined from the force displacement relationship obtained from the previous quasi-static tests on similar type of isolators.

The linearized procedure uses effective stiffness and effective damping to characterize the nonlinear properties of isolators. Eurocode [21] permits modeling of the isolation system with an equivalent

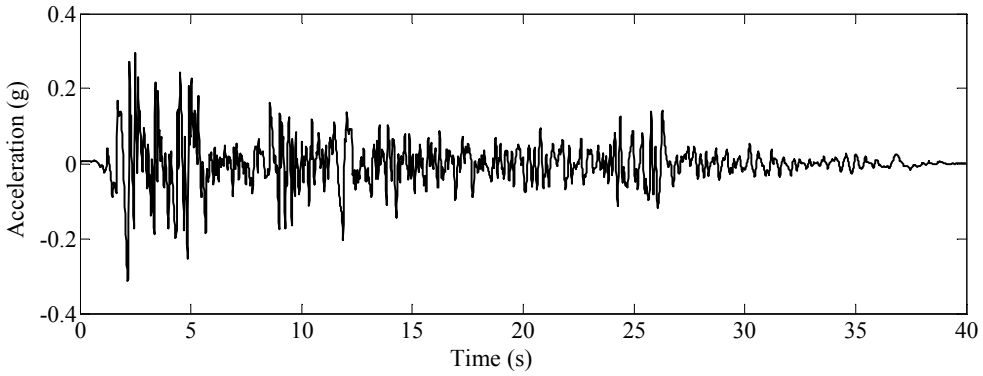

Fig. 10 Input accelerogram (El Centro 1940, NS component, PGA = 0.313 g).

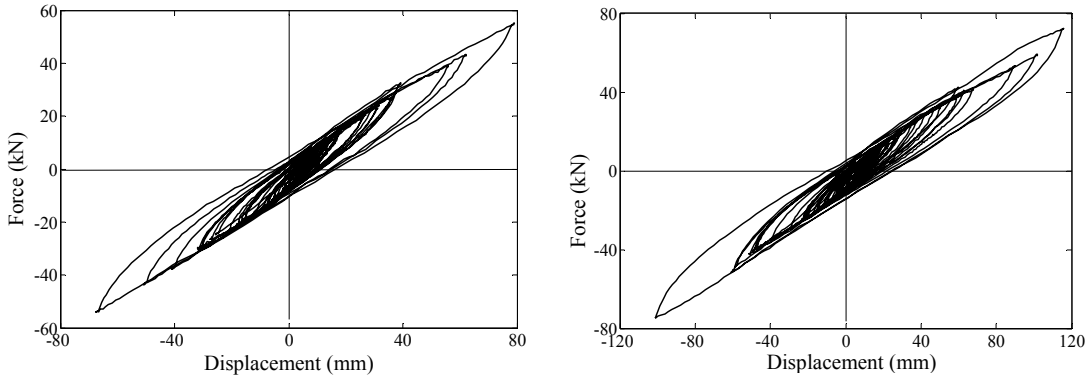

(a) 100% El Centro NS input case (b) 150% El Centro NS input case

Fig. 11 Force displacement relationship of STRP-4.

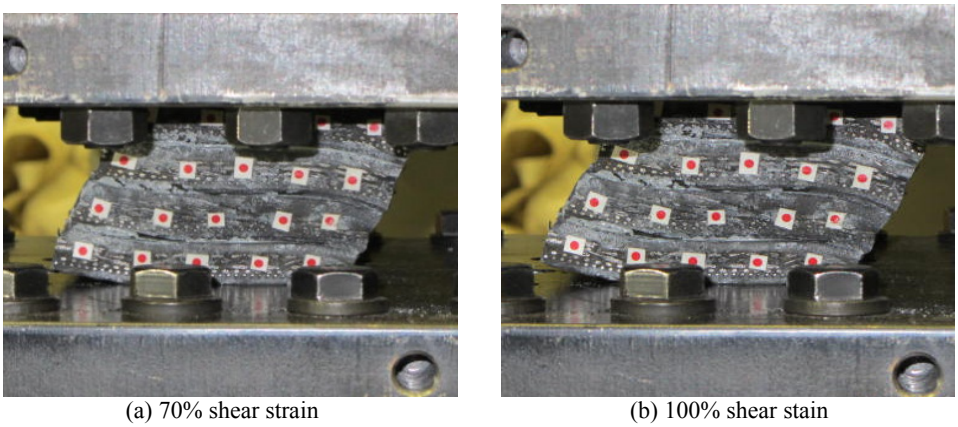

(a) 70% shear strain (b) 100% shear stain

Fig. 12 Deformed state of STRP-4 observed during pseudodynamic test.

linear elastic-viscous behavior, if it consists of devices such as laminated elastomeric bearings. When an equivalent linear model is used, the effective stiffness of each isolator unit should be used, and energy dissipation of the isolation system should be expressed in terms of an equivalent viscous damping as the effective damping. Similarly, FEMA [22] permits linear procedures with certain limitations. Although the static response of a structure supported on a system of this type shows a bilinear hysteretic restoring force behavior [23], equivalent linear elastic models are often used in order to simplify the design and analysis of seismically isolated buildings, at least at the preliminary design and analysis phase [24]. According to Uniform Building Code [15], the nonlinear-force deformation characteristic of the isolator can be

replaced by an equivalent linear model through effective elastic stiffness and viscous damping. In the current design practices for seismically isolated structures, an equivalent linear elastic structure with an effective period and an equivalent viscous damping ratio accounting for energy dissipation due to inelastic deformation of isolator is usually used for preliminary design [25]. Mavronicola et al. [24] concluded that the equivalent linear analysis may be used under certain limitations for the preliminary design and analysis of a seismically isolated building. Bilinear modeling would produce better result if the yield displacement and corresponding force could be determined with a good accuracy. However, unlike the other virgin rubbers, determination of yield displacement of STRP is difficult.

The governing equation of motion for the base isolated structure can be written as Ref. [26]

$$[M_s]\{\ddot{x}\} + [C_s]\{\dot{x}\} + [K_s]\{x\} = -[M_s]\{r\}(\ddot{x}_b + \ddot{x}_g) \quad (9)$$

where, M_s, K_s and C_s are the mass, stiffness and damping matrices of the superstructure. x, $\dot{x}$ and $\ddot{x}$ are the displacement, velocity and acceleration vectors of the superstructure, respectively, $\ddot{x}_g$ and $\ddot{x}_b$ are the excitation acceleration and acceleration of bass floor, respectively, and r represents the influence coefficient vector.

The corresponding equation of motion for the base mass under earthquake ground motion is expressed by:

$$m_b\ddot{x}_b + F_b - c_1\dot{x}_1 - k_1x_1 = -m_b\ddot{x}_g \quad (10)$$

where, m_b is the base floor mass, F_b is the restoring force of isolation system, c_1 and k_1 are the first story damping and stiffness, respectively. In Eq. (10), mass and stiffness matrices are known but the damping matrix of the superstructure is not known explicitly. The STRP bearings were modeled by using equivalent linear elastic viscous damping model. The linear force developed in the isolation system can be expressed as:

$$F_b = k_{eff}\,x_b + c_{eff}\,\dot{x}_b \quad (11)$$

where, k_{eff} and c_{eff} are the effective stiffness and effective damping value of the isolation system.

The damping matrix C_s of the superstructure has to generate either by using the modal damping or by using Rayleigh damping [27].

In this model, first and fourth modes were used to define the superstructure's damping matrix with 5% critical damping. The overall damping matrix C is obtained by assembling the damping matrices of the superstructure and the isolation system. As the time integration scheme, Newmark's β method with $\beta = 1/6$ and $\gamma = 1/2$ with the time step interval of Δt = 0.001 s was used.

6. Comparison between Pseudo-dynamic Test and Numerical Analysis Results

The results of the pseudo-dynamic tests and numerical analysis are described. Fig. 13 shows the comparison between the numerical analysis and pseudo-dynamic tests results in terms of the force-displacement behavior.

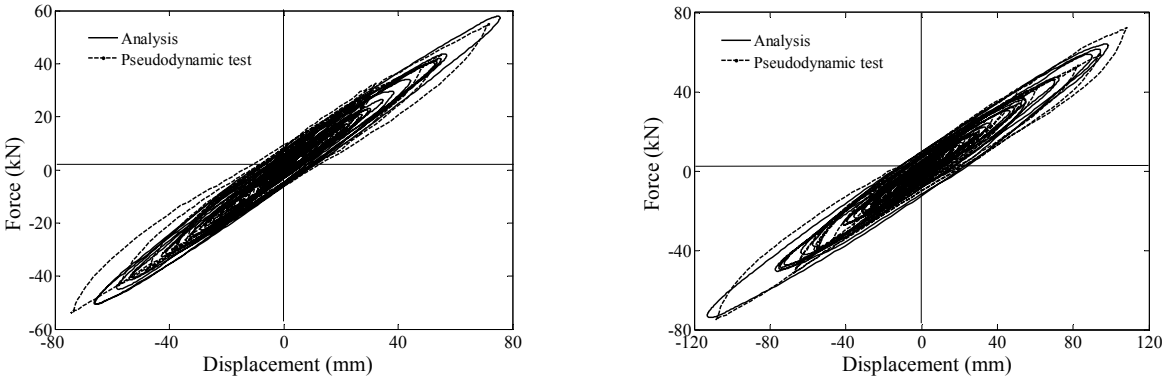

(a) 100% El Centro input case (b) 150% El Centro input case

Fig. 13 Force-displacement relationship of STRP isolator: comparison between pseudodynamic test and numerical analysis results.

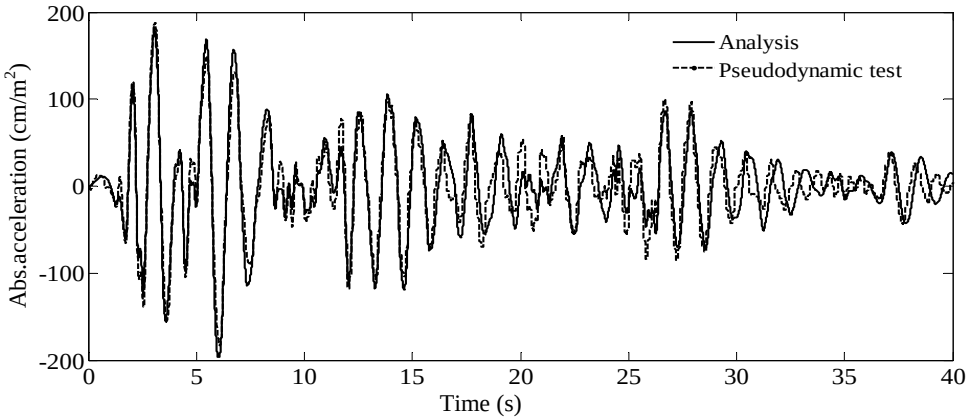

Fig. 14 Top floor absolute acceleration time history, 100% El Centro NS input case.

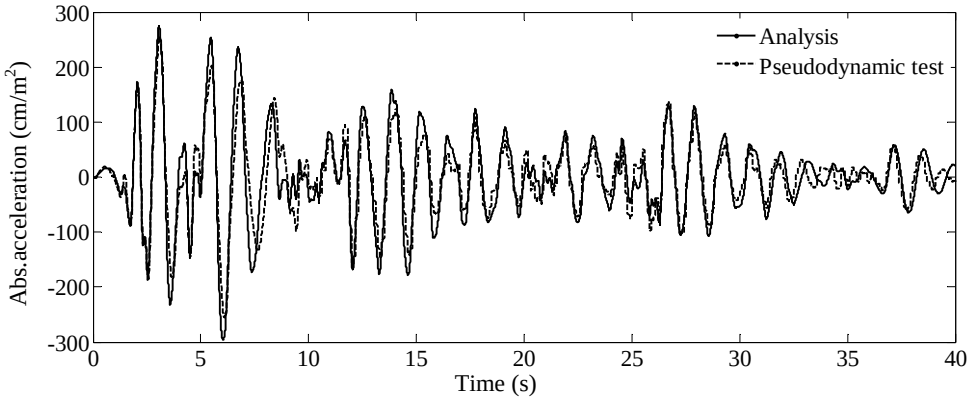

Fig. 15 Top floor absolute accelerations time history, 150% El Centro NS input case.

Table 6 Floor drifts obtained by pseudodynamic tests and analysis.

Floor level	Floor drift (mm)			
	100% El Centro NS input		150% El Centro NS input	
	Pseudodynamic test	Simulation	Pseudodynamic test	Simulation
First	7.9	7.9	10.4	12.10
Second	5.1	5.24	6.9	7.87
Roof	2.3	2.44	3.1	3.64

Table 7 Maximum absolute floor accelerations (cm/s^2).

Method	Base	First	Second	Roof
El Centro 100%				
1. Pseudodynamic test	164.0	172.0	183.0	187.0
2. Numerical simulation	175.8	187.5	193.7	197.1
El Centro 150%				
1. Pseudodynamic test	224.0	236.0	249.0	255.0
2. Numerical simulation	263.7	281.1	290.6	295.6

A close agreement between the numerical analysis and the pseudo-dynamic test results can be seen in these plots.

Comparison of the floor drifts obtained by numerical analysis and the pseudo-dynamic tests is shown in Figs. 14 and 15 and summarized in Table 6. It can be seen in Table 6 that the floor drifts obtained by numerical analysis and pseudo-dynamic tests are almost equal for

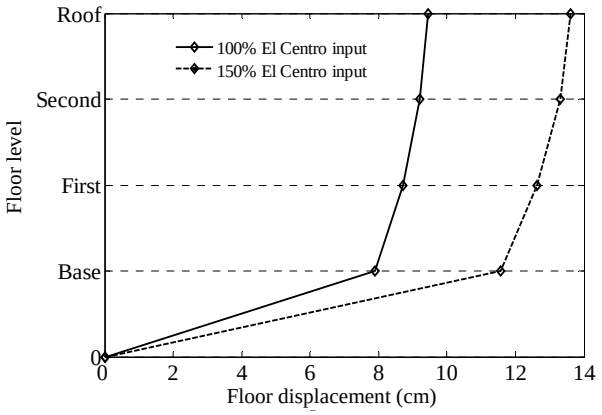

Fig. 16 Comparison of floor displacements profile for different input amplitude level.

100% El Centro input case, while the difference is noticeable for the case of an increased level of excitation with the scale factor of 1.5. Situation is similar for the top floor absolute acceleration, as shown in Table 7. Although the effective stiffness of the STRP isolator decreases with increase in lateral displacement, a constant effective stiffness value is determined for 120% shear strain is used in the dynamic analysis of the STRP isolator, resulting in higher displacement demand. Since the damping ratio is also dependent on shear strain as shown in Fig. 6, use of a constant effective damping ratio may lead to discrepancy between the test and analysis results. Fig. 16 shows the floor displacement profile obtained by the pseudodynamic test. These results indicate that the equivalent linear elastic-viscous damping model overestimate the displacement demand which can be considered appropriate for preliminary analysis and design of STRP isolators.

A greater difference between the pseudodynamic test results and simulation results is observed for the case of the increased input acceleration amplitude. The maximum difference is found for roof level absolute acceleration which is about 15% higher than the pseudodynamic test result. From Tables 6 and 7, it can be concluded that the floor acceleration obtained by numerical simulation is slightly higher than the pseudodynamic test result in all cases. There may be substantial increase in the top floor acceleration as the fundamental period of the superstructure increases. In this analysis, superstructure is considered as rigid.

7. Comparison between Fixed Base and Base Isolated Case

The pseudodynamic tests results are further compared with the results of analysis of the fixed base case for the identical building. The seismic performance of the isolated building is evaluated in terms of absolute acceleration, drift and base shear. The comparative response time histories are presented in Figs. 17-19. The comparison of floor drifts for fixed base and base isolated buildings for the two levels of 100% and 150% El Centro record excitation is also shown in Fig. 20. An important index for the performance evaluation of the base isolation system is the peak inter-story drift. In this case, the inter-story drift at the top is reduced with approximately 81%, which is within the limit of $0.02/R_I$ as designed [15]. The base shear force transmitted to the superstructure

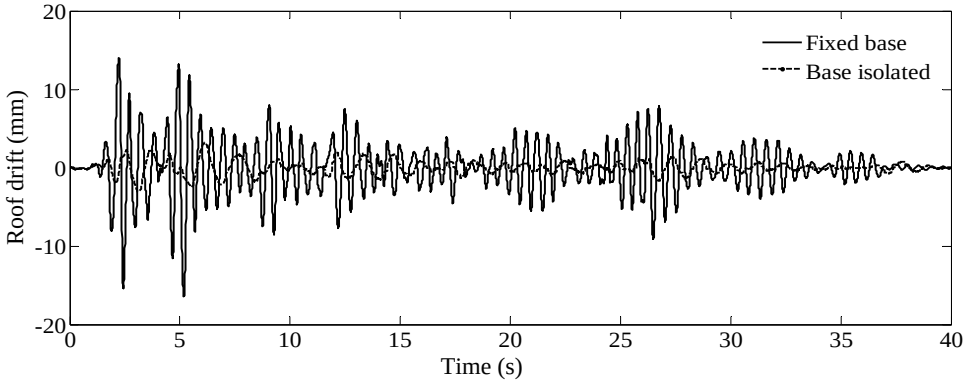

Fig. 17 Top floor drift: comparison between numerical analysis of fixed base case and pseudodynamic test of base isolation case.

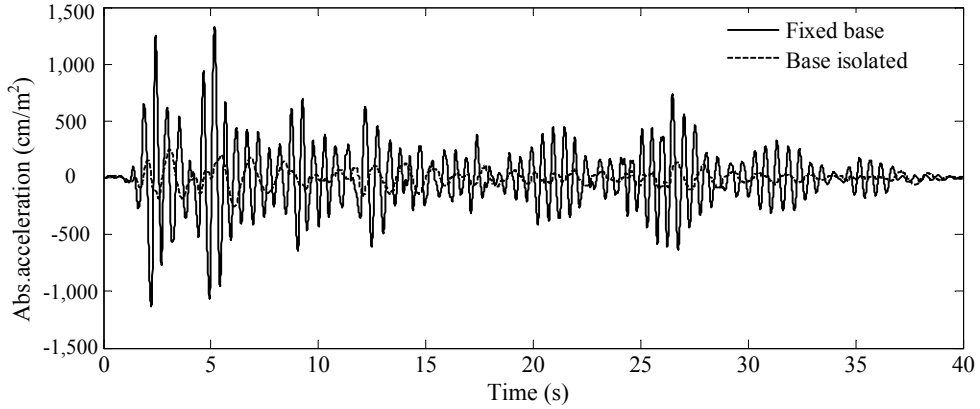

Fig. 18 Top floor absolute acceleration: comparison between numerical analysis of fixed base case and pseudodynamic test of base isolation case.

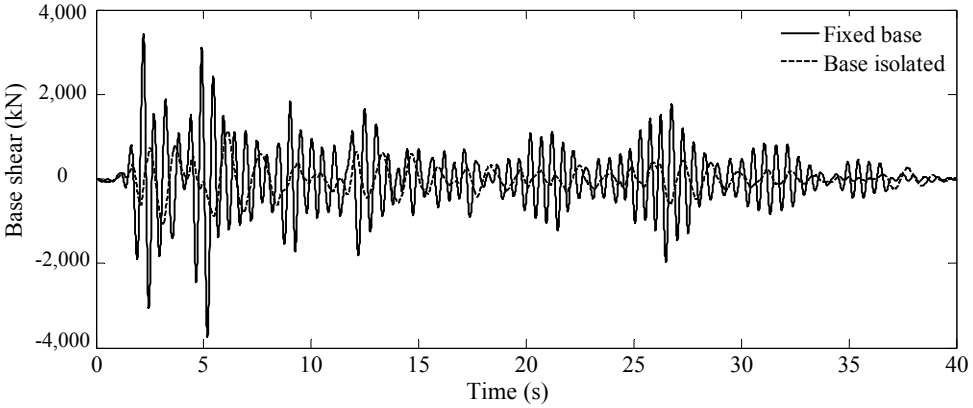

Fig. 19 Base shear: comparison between numerical analysis of fixed base case and pseudodynamic test of base isolation case.

for fixed base and base isolation cases are 3,740 kN and 1,124 kN, respectively. These results indicate that the reduction of base shear due to base isolation is as much as 70% of that for the fixed base case. It can be concluded that, on an average, numerical analysis of the fixed base case predicts 15% higher top floor drifts and 13% higher top floor absolute accelerations compared with the building with the base isolation. Considering these variations, one can conclude that the reduction of top floor drifts, top floor absolute accelerations and base shear are 66%, 67% and 70%, respectively.

8. Conclusions

As a part of the development of a low-cost seismic isolation system, seismic performance of a building with seismic isolators using scrap tire rubber pad is verified by means of the pseudo-dynamic test in this study. Although accurate numerical modeling of the dynamic behavior of tire rubber pads by analytical methods is difficult, dynamic response of the base

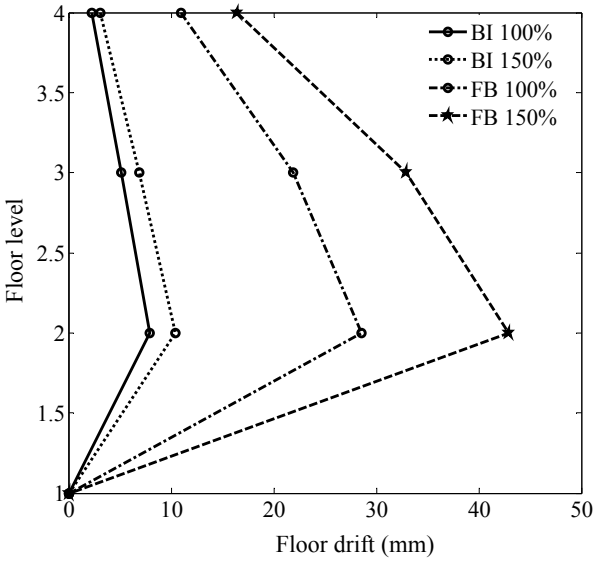

Fig. 20 Floor drift profile in fixed base and base isolation cases under 100% and 150% El Centro NS record input.

isolation system as well as seismic performance of a three story base isolated building using STRP isolators can be evaluated while avoiding the problems associated with shaking table tests.

The isolators used in this study were produced by using scrap tire rubber pads. Due to the capacity of testing equipment available, 1/3 scale isolator models were used as the specimens in the pseudo-dynamic test. The mechanical properties of the tested isolators were determined by conducting quasi-static cyclic loading tests. Seismic performance of the base isolated building was evaluated for two levels of seismic excitation: The El Centro record scaled with 100% and 150% amplitudes corresponding to the PGA values of 0.313 g and 0.47 g, respectively.

The maximum responses obtained from numerical simulation were found to be in reasonable agreement with pseudodynamic tests results. The seismic performance of the base isolated building was evaluated in terms of absolute acceleration, drift, base shear and isolator's displacement compared with numerical simulation results for the fixed base building. In this case, the reduction of the top floor inter-story drift and absolute acceleration are approximately 66% and 67%, respectively, and base shear force transmitted to the superstructure is reduced to 70% of that for the fixed base building, showing that the top floor drift is within the limit of $0.02/R_I$. These results indicate that the base isolation system using STRP isolators is an attractive alternative to commercially available isolation systems.

References

[1] L. di Sarno, E. Chioccarelli, E. Cosenza, Seismic response of an irregular base isolated building, Bulletin of Earthquake Engineering 9 (5) (2011) 1673-1702.

[2] J.M. Kelly, Seismic isolation system for developing countries, Earthquake Spectra 18 (3) (2002) 385-406.

[3] H. Toopchi-Nezhad, M.J. Tait, R.G. Drysdale, Testing and modeling of square carbon fiber-reinforced elastomeric seismic isolators, Structural Control and Health Monitoring 15 (6) (2008) 876-900.

[4] J.M. Kelly, D. Konstantinidis, Low-cost seismic isolators for housing in highly-seismic developing countries, in: 10th World Conference on Seismic Isolation, Energy Dissipation and Active Vibrations Control of Structures, Istanbul, Turkey, May 2007, pp. 28-31.

[5] A. Mordini, A. Strauss, An innovative earthquake isolation system using fiber reinforced rubber bearings, Engineering Structures 30 (10) (2008) 2739-2751.

[6] A. Turer, B. Özden, Seismic base isolation using low-cost scrap tire pads (STP), Materials and Structures 41 (5) (2008) 891-908.

[7] H.K. Mishra, A. Igarashi, H. Matsushima, Finite element analysis and experimental verification of the scrap tire rubber pad isolator, Bulletin of Earthquake Engineering 11 (2013) 687-707.

[8] H.K. Mishra, I. Akira, Lateral deformation capacity and stability of layer-bonded scrap tire rubber pad isolators under shear loading, Bulletin of Earthquake Engineering. (in print)

[9] J.E. Carrion, B.F. Spencer, B.M. Philips, Real-time hybrid testing of a semi-actively controlled structure with an MR damper, in: American Control Conference, USA, 2009.

[10] A.P. Darby, A. Blakeborough, M.S. Williams, Real-time substructure tests using hydraulic actuator, Journal of Engineering Mechanics 125 (10) (1999) 1133-1139.

[11] H. Krawinkler, Scale effects in static and dynamic model testing of structures, in: Proceedings of Ninth World Conference on Earthquake Engineering, Japan, 1988.

[12] A. Souid, A. Delaplace, F. Ragueneau, R. Desmorat, Pseudodynamic testing and nonlinear substructuring of damaging structures under earthquake loading, Engineering Structures 31 (5) (2009) 1102-1110.

[13] S.A. Mahin, P.B. Shing, Pseudodynamic method for seismic testing, Journal of Engineering Structures 111 (7) (1985) 1482-1503.

[14] S.K. Jain, S.K. Thakar, Quasi-static testing of laminated rubber bearings, Journal of the Institution of Engineers (India), Civil Engineering Division 84 (2003) 110-115.

[15] Earthquake Regulations for Seismic Isolated Structure, Structural Design Requirements, Vol. 2, Uniform Building Code (UBC 1997), Whittier, CA, 1997.

[16] J.M. Kelly, Earthquake-Resistant Design with Rubber, 2nd ed., Springer-Verlag, London, 1997.

[17] Y.J. Arditzoglou, J.A. Yura, A.H. Haines, Test Methods for Elastomeric Bearing on Bridges, Texas Department of Transportation, Research report 1304-2, 1995.

[18] H. Holcher, M. Tewes, N. Botkin, M. Lohndorf, K.H. Hoffmann, E. Quandt, Modeling of pneumatic tires by a finite element model for the development of a tire friction remote sensor, Technical Paper, Center of Advanced European Studies and Research (Caesar), 2004, p. 40.

[19] N.S. Kim, J.H. Lee, S.P. Chang, Equivalent multi-phase similitude law for pseudodynamic test on small scale reinforced concrete models, Engineering Structures 31 (4)

(2009) 834-846.

[20] Nepal National Building Code, NBC 105, 1994.

[21] Design of Structures for Earthquake Resistance, Eurocode 8, UK, 2004.

[22] Federal Emergency Management Agency FEMA 273, the National Earthquake Hazards Reduction Program (NEHRP) Guidelines for Seismic Rehabilitation of Buildings,1997.

[23] R.I. Skinner, J.A. Beck, G.N. Bycroft, A practical system for isolating structures from earthquake attack, Earthquake Engineering and Structural Dynamics 3 (3) (1975) 297-309.

[24] E. Mavronicola, P. Komodromos, Assessing the suitability of equivalent linear elastic analysis of seismically isolated multi-story buildings, Computers and Structures 89 (21-22) (2011) 1920-1931.

[25] X.Z. John, J. Zhang, Inelastic demand spectra for bilinear seismic isolation systems based on nonlinear time history analysis and the response of lead-rubber bearing isolation systems subjected to near-source ground motions, Bulletin of the New Zealand Society for Earthquake Engineering 40 (1) (2007) 7-17.

[26] V.A. Matsagar, R.S. Jangid, Influence of isolator characteristics on the response of base-isolated structures, Engineering Structures 26 (2003) 1735-1749.

[27] K.L. Ryan, J. Polanco, Problems with Rayleigh damping in base-isolated buildings, Journal of Structural Engineering 134 (11) (2008) 1780-1784.